

# A Dipole Magnet for the FRIB High Radiation Environment Nuclear Fragment Separator

S. A. Kahn, M. Anerella, A. Dudas, G. Flanagan, R. C. Gupta, J. Nipper, and J. Schmalzle

**Abstract**—Magnets in the fragment separator region of the Facility for Rare Isotope Beams (FRIB) would be subjected to extremely high radiation and heat loads. The critical elements of FRIB are the dipole magnets, which are used to select the desired isotopes. Since conventional NiTi and Nb<sub>3</sub>Sn superconductors must operate at  $\sim 4.5$  K, the removal of the high heat load generated in these magnets using these superconductors would be difficult. High-temperature superconductors have been shown to be radiation resistant and can operate in the 40 K temperature range where heat removal is an order of magnitude more efficient than at 4.5 K. The coils of this magnet must accommodate the large curvature from the 30° bend that the magnet will subtend. This paper will describe the magnetic and conceptual design for these magnets.

**Index Terms**—High-temperature superconductor (HTS), HTS coils, HTS magnets.

## I. INTRODUCTION

THE FRIB facility at MSU will provide isotope beams for physics research with intensities not available elsewhere [1]. The facility will enable scientists to study the properties of nucleonic matter providing insight into the nuclear processes in stars as well as test fundamental symmetries in nuclear physics. Large quantities of various isotopes are produced when a high power 400 kW linac beam hits the target. FRIB will have the ability to accommodate various primary beams from protons to uranium with energies up to 200 MeV/u. The beams will be incident on a carbon target to produce a variety of secondary nuclides with various ionic charge states. The fragment separator which follows the target consists of a series of three quadrupole magnets to provide focusing and two dipole bend magnets to select the desired nuclei. The beam enters the first dipole magnet with a spread of rigidities. The undesired nuclides are removed with a beam dump between the two dipole magnets.

As the production rate for a specific rare isotope can be very small, the magnets in the fragment separator will have large apertures and strong magnetic fields to maximize the collection of these rare isotopes. The radiation level in the fragment separator magnets is quite high and these magnets need to be ra-

Manuscript received July 15, 2013; accepted September 3, 2013. Date of publication September 6, 2013; date of current version October 12, 2013. This work was supported in part by the U.S. Department of Energy under Grants DE-SC-0006273 and DE-AC02-98CH10886.

S. A. Kahn, A. Dudas, G. Flanagan, and J. Nipper are with Muons, Inc., Batavia, IL 80510 USA (e-mail: kahn@muonsinc.com).

M. Anerella, R. C. Gupta, and J. Schmalzle are with Brookhaven National Laboratory, Upton, NY 11973 USA.

Color versions of one or more of the figures in this paper are available online at <http://ieeexplore.ieee.org>.

Digital Object Identifier 10.1109/TASC.2013.2281031

TABLE I  
DESIGN PARAMETERS FOR THE FRAGMENT SEPARATOR DIPOLE MAGNET

Parameter	Value
Bending Radius	4 m
Bend Angle	30°
Magnetic Length along Beam Path	2.094 m
Nominal Central Field	2.0 T
Operating Field Range	0 to 2.2 T
Field Non-Uniformity in Good Field Region	<0.7 %
Good Field Width in Bend Plane	0.3 m
Good Field Height in Non-Bend Plane	0.2 m
Total Current Required in Each Coil	256 kA-turns
Operating Temperature	40 K

diation resistant. The radiation dose seen by the first quadrupole after the target is estimated to be  $2.5 \times 10^{15}$  neutrons/cm<sup>2</sup> per year (10 MGy/year) [2] which corresponds to 10 kW/m of deposited power. The deposited power will drop by an order of magnitude before reaching the first bending dipole. The high radiation environment influences the magnet design and the choice of materials used. Although NiTi and Nb<sub>3</sub>Sn are robust conductor materials in radiation, they must operate at 4.5 K which is not practical, since the anticipated heat load would be difficult and expensive to remove at that temperature. HTS conductors are reasonably resistant against radiation and have a significant current density at 40 K where the heat capacity of the refrigerants is much larger and the Carnot efficiency is greater making heat removal easier.

Brookhaven National Laboratory has been involved in an R&D program to develop the quadrupole magnets for pre-fragment separator at FRIB [3]–[6] using HTS conductor. The design of the fragment separator dipole magnets will rely on the technology that was learned.

## II. MAGNETIC DESIGN

The design parameters of the fragment separator dipole magnet are shown in Table I. There are two such magnets in the fragment separator which is used to select the desired nuclide. Each of these magnets bends the beam by 30° with a nominal field of 2 T. The magnet should have field uniformity better than 0.7% over the useful beam aperture for operating field between 0.5 and 2.0 T. We have chosen a superferric design for this magnet where HTS coils are used to magnetize the iron which provides the desired field. The coils surround the iron poles and are enclosed in their cryostat. The coil and cryostat package are recessed behind the iron pole to protect them from a direct exposure to the radiation from the beam however the main source of radiation is from neutrons which will penetrate into the coils. Most of the radiation and associated heat

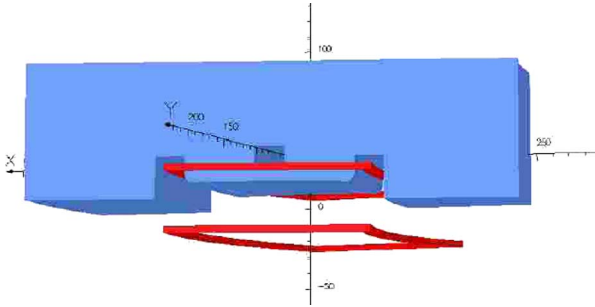


Fig. 1. Model of the upper quarter of the magnet geometry.

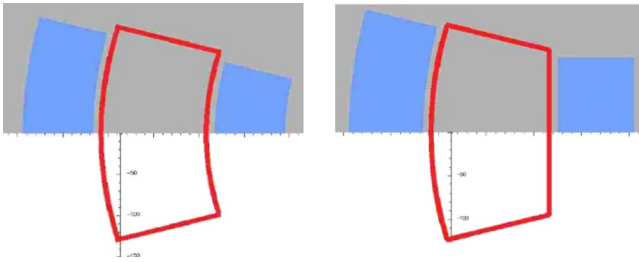


Fig. 2. Two-coil configurations that have been examined. The left diagram uses a curved inner radius coil, which is wound with negative curvature. The right diagram uses straight conductor for that segment of the coil.

generated will be deposited into the iron yoke which is at room temperature. It is estimated that  $\sim 1$  kW will be deposited into coil cryostats. Fig. 1 shows a sketch of the sector bend magnet where only one half of the upper half of the iron is shown. The upper and lower coils must each carry 256 kA-turns to produce the design 2 T field in the beam aperture.

### III. SUPERCONDUCTING COILS

We plan to wind the coils with YBCO conductor which will be operated at 40 K. The coils are located at a position where the field will be  $\sim 2.5$  T with comparable radial and vertical components. As the critical current of YBCO conductor is sensitive to the local direction of the field we must design for the field component perpendicular to the conductor plane which has a lower critical current. To provide a safe margin against quenching the coils should be operated at two-thirds of the critical current at 40 K and in the  $B_{\perp} = 2.5$  T field. We expect that we can obtain 400 A using Super Power 12 mm (SCS 12050-AP) conductor under these conditions [7]. The coils will need 5.5 km of this conductor for the magnet.

An important consideration in the winding of the coils is that the field must preserve the transverse 2D profile. The left diagram in Fig. 2 shows a configuration where the inner radius segment of the coil is wound with negative curvature which is more difficult since the conductor will tend to spring back and unwind. Each turn must be constrained to avoid this from happening. A 1/4 scale test coil with this configuration using the negative curvature segment was wound [8] and successfully tested. It was however necessary to use epoxy to hold the conductor turns together during the coil winding. We would like to minimize the use of epoxy on this magnet since organic materials can deteriorate in the radiation environment. The sketch on the right side of Fig. 2 shows the chosen coil geometry with

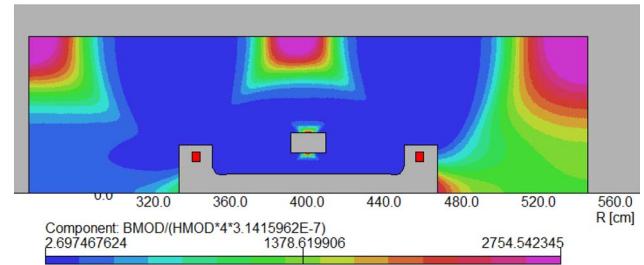


Fig. 3. Relative permeability of the iron yoke is shown.

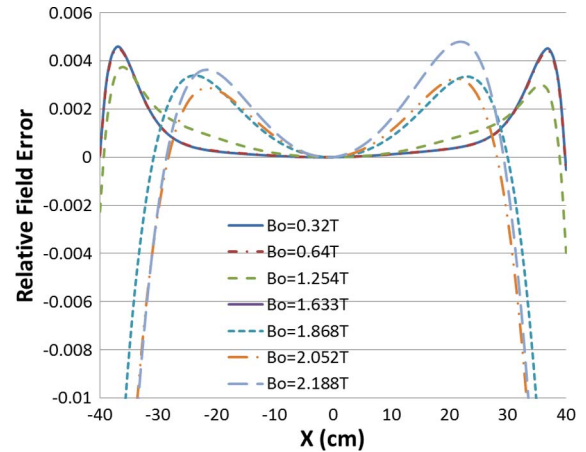


Fig. 4. Relative field error,  $\Delta B/B$ , as a function of position in the aperture. Curves are shown for different central fields ranging from 0.23 to 2.188 T.

the inner radial straight segment. The role of the coil in a superferric magnet is to magnetize the iron which determines the field quality. The two configurations shown in the Fig. 2 were compared using the Tosca 3-D EM finite element program. The fields of the two configurations differ by less than 1% in the good field region, which can be corrected by shaping the pole.

### IV. FIELD CALCULATIONS

The field error,  $\Delta B/B$ , should be less than 0.7% for the operating field range from 0.7 to 2.0 T over the good field region defined in Table I. This is achieved by controlling the magnetization in the magnet yoke. Fig. 3 shows the relative permeability in the iron. The iron on the smaller radius inner side shows more saturation than on the larger radius outer side. The rectangular hole in the hole is placed to effectively control the saturation. Fig. 4 shows  $\Delta B/B$  as a function of transverse position in the aperture for various field excitations. The field error is less than 0.7% for all values of  $B_0$  in the region  $\pm 30$  cm from the magnet center.

### V. THERMAL AND STRUCTURAL ISSUES

The coils will feel substantial Lorentz forces when the magnet is fully energized. Table II shows the coil forces at the 2.0 T operating field and at the 2.2 T maximum design field. The large forces shown in Table II will require substantial mechanical support to minimize coil movement when the coils are powered. A preliminary study which attempts to constrain the coil forces with a support structure entirely within the cryostat produced

TABLE II  
LORENTZ FORCES PER UNIT LENGTH ON THE COIL

Field	Coil	$F_{\text{radial}}/\text{Length}$	$F_{\text{vertical}}/\text{Length}$
Tesla		N/m	N/m
2.0	Outer	120735	105252
	Inner	-108828	108512
2.2	Outer	167079	112226
	Inner	-146093	117935

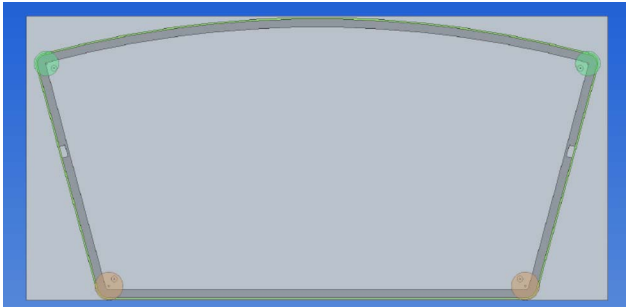


Fig. 5. Sketch of the winding bobbin attached to the back plate support.

coil deflections that were too large. External support that would penetrate into the cryostat and be anchored to the pole or flux return iron will be necessary. By using an external support the coil deflections are reduced significantly and the mechanical stress on the coil is reduced to 41 MPa which is acceptable. This approach will introduce some heat leaking into the cryostat. The design of the coil support will need to minimize the coil movement while also minimizing the heat generated.

## VI. TEST COIL PROGRAM

A test coil is being constructed as part of an R&D effort for the magnet design. The test coil will be full sized, wound with YBCO conductor, however will have fewer turns to make it affordable with the resources available. The program will develop manufacturing techniques for winding and handling the large coils. It will also demonstrate that the coil can operate in a steady state condition with the anticipated heat load expected for the radiation environment in this magnet. In the test program we will develop the winding tooling and the cryogenic cold mass. The winding tooling shown in Fig. 5 is comprised of the winding bobbin which is attached to a back plate for support. As the winding bobbin is relatively thin it is attached to a back plate to support it during the winding and assembly process. The conductor tape is wound around the outer surface of the bobbin using 6.5 m of conductor for each turn. Two coils are wound on their respective bobbins and put together in a double coil assembly. The back plate is necessary to facilitate the moving and rotation of these large coil packages with minimal coil distortion. The conductor on each of the two coils is wound with the opposite sense of rotation so that the coils can be connected in series at the inner conductor attachment slots. The coils wound in this manner will have the same current direction. Table III shows the parameters describing the bobbin. After the two coils are assembled together the back plates are removed.

Additional tooling will be added to the wound two coil assembly for cooling of the coils and mechanical support. Fig. 6 shows the cross section sketch of the wound coils with

TABLE III  
PARAMETERS DESCRIBING THE WINDING BOBBIN AND COLD MASS

Parameter	Value
Overall Length w/Coils	241.72 cm
Overall Width w/Coils	120.81 cm
Bobbin Depth	1.27 cm
Bobbin Thickness	3.5 cm
Orbit Curvature	4 m
Curvature of Outer Bobbin Surface	4.54 m
Pole Angle	30°
Distance between Coil and Iron Pole	3.9 cm

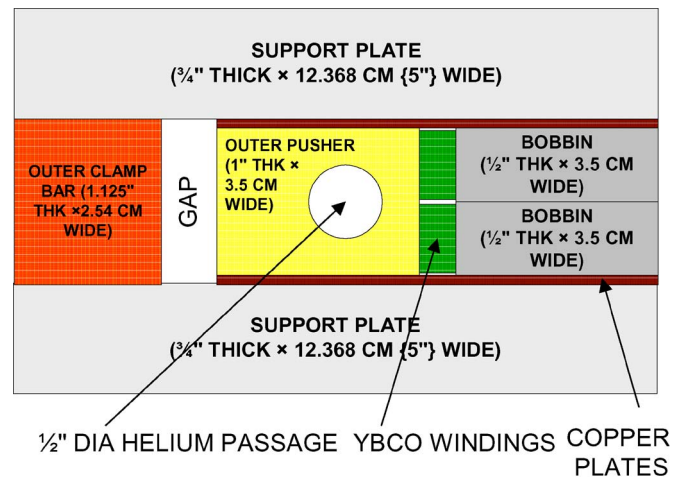


Fig. 6. Cross-section of the double coil inside the support and cooling structure.

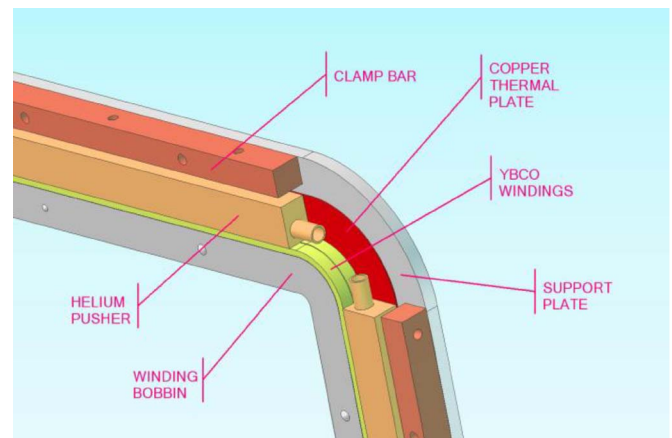


Fig. 7. Open view of the double coil plus assembly structure with parts marked. Support plate on near side is removed to make inner parts visible.

the associated tooling. Outside the coils is a stainless steel support followed by a cooling section containing a hole for pressurized helium gas (referred to as outer pusher in the figure). The cooling channel will likely be made of stainless steel to match the expansion coefficient of the support structure. We have examined the use of copper for the cooling channel because of its superior thermal conductivity. This would have lowered the steady state temperature at the conductor by 2° and might be available commercially, although we could not find hollow copper conductor available in the desired dimension. We have chosen stainless steel because of its superior strength and will gun drill the cooling aperture. Because of the size of the coil mass structure it will likely be necessary to assemble

shorter pieces that will be welded together. Heater strips will be inserted during the winding to simulate the heat load. The helium flow rate and pressure will be adjusted to maintain the coils at the operating temperature. Fig. 7 shows an open view of the two coil assembly with support and cooling structures. The front plate is omitted to make the inner parts visible.

## VII. CONCLUSIONS

This paper describes a conceptual design of a dipole magnet for the FRIB fragment separator. This magnet will operate in a high radiation environment which puts constraints on the design. The approach is to use a superferric design with HTS conductor that can be operated at 40 K where the heat generated by radiation can be efficiently removed. The design of the coil support must accommodate minimum coil displacement from Lorentz forces, must minimize mass so as to reduce heat generation and must minimize the heat introduced into the cold mass. The R&D program will address these design issues.

## REFERENCES

- [1] [Online]. Available: <http://www.frib.msu.edu>
- [2] A. F. Zeller, "Superconducting magnets for RIA," in *Proc. Adv. Cryogenic Eng.*, 2004, vol. 49A, pp. 758–765.
- [3] R. Gupta, M. Anerella, M. Harrison, W. Sampson, J. Schmalzle, R. Ronningen, and A. Zeller, "Radiation resistant HTS quadrupoles for RIA," *IEEE Trans. Appl. Supercond.*, vol. 15, no. 2, pp. 1252–1255, Jun. 2005.
- [4] R. Gupta, M. Anerella, A. Ghosh, J. Schmalzle, and W. Sampson, "Design, construction, test results of a warm iron HTS quadrupole for the facility for rare isotope beams," *IEEE Trans. Appl. Supercond.*, vol. 18, no. 2, pp. 236–239, Jun. 2008.
- [5] S. Chouhan, D. Cole, J. DeKamp, C. Wilson, and A. F. Zeller, "Radiation resistant superferric quadrupole magnets with warm iron," *IEEE Trans. Appl. Supercond.*, vol. 21, no. 3, pp. 1813–1816, Jun. 2011.
- [6] R. Gupta, M. Anerella, J. Cozzolino, G. Ganetis, A. Ghosh, G. Greene, W. Sampson, Y. Shiroyanagi, P. Wanderer, and A. Zeller, "Second generation HTS quadrupole for FRIB," *IEEE Trans. Appl. Supercond.*, vol. 21, no. 3, pp. 1888–1891, Jun. 2011.
- [7] S. A. Kahn and R. C. Gupta, "High radiation environment nuclear fragment separator dipole magnet," in *Proc. IPAC12*, 2012, pp. 3605–3607.
- [8] S. A. Kahn, R. C. Gupta, G. Jochen, Y. Shiroyanagi, and S. A. Kahn, "Fabrication and testing of curved test coil for FRIB fragment separator dipole," in *Proc. IPAC12*, 2012, pp. 3611–3613.